Korean J. Chem. Eng., **24**(5), 866-871 (2007)

Pressure fluctuations and bubble size in viscous three-phase circulation fluidized bed bioreactors

Sung Mo Son, Ik Sang Shin, Suk Hwan Kang, Yong Kang† and Sang Done Kim*

School of Chemical Engineering, Chungnam National University, Daejeon 305-764, Korea
*Department of Biomolecular & Chemical Engineering, KAIST, Daejeon 305-701, Korea
(*Received 9 August 2006 • accepted 1 February 2007*)

Abstract−Characteristics of pressure fluctuations and bubble size were investigated in the riser of a three-phase circulation fluidized bed bioreactor with viscous liquid medium, whose diameter is 0.102 m (ID) and 3.5 m in height. Effects of gas (0.01-0.07 m/s) and liquid (0.17-0.23 m/s) velocities and liquid viscosity (0.96-38 mPa·s) on the bubble size in the riser were examined. The bubbling phenomena in the bioreactor with viscous liquid medium were interpreted effectively by measuring and analyzing the pressure fluctuations by adopting chaos theory. The bubble size increased with increasing gas velocity or liquid viscosity, but decreased with increasing liquid velocity. The bubbling phenomena became more complicated and bubble size distribution tended to broad, with increasing gas velocity or liquid viscosity. The bubble size was well correlated in terms of correlation dimension of pressure fluctuations as well as dimensionless groups within these experimental conditions.

Key words: Pressure Fluctuations, Viscous Bioreactor, Bubble Size, Three-phase Circulation, Chaos Analysis

INTRODUCTION

For the practical applications of three-phase fluidized beds, a three-phase circulation fluidized bed has been proposed, since it can be utilized successfully as a reactor or a contactor when small or light particles and suspensions are fluidized in a viscous liquid medium, which is often encountered in environmental, biochemical and food processing engineering. The three-phase circulation fluidized bed can minimize the dead zone in the column as well as increase the contacting efficiency among gas, liquid and solid phases. These advantages can lead to considerable increases in the fractional conversion as well as production efficiency per unit cross-sectional area of the system [1-6]. Moreover, the deactivated catalyst, bio-media, ion exchange resin, or adsorbent can be regenerated continuously by means of the solid circulation mode between the main reactor or contactor (riser) and the regenerator (downcomer).

It is understood that the information on the flow and bubbling behaviors of gas phase is known to a play critical role in determining the oxygen transfer in the bioreactors, since the bubbles which exist as a dispersed phase are flowing stochastically and randomly in the viscous liquid medium [7-13]. However, little attention has been focused on the bubbling phenomena in three-phase circulation fluidized bed bioreactors [14-16], especially in reactors with a viscous liquid medium such as wastewater from food processing industries. Recently, the complicated nonlinear multiphase flow and contact phenomena have been successfully described by adopting the chaos theory. That is, the conglomerating effects of multiple dynamic phenomena such as bubbling behavior in multiphase flow systems can be analyzed conveniently by means of chaotic parameters such as attractor or dimension [17-21].

In the present study, thus, pressure fluctuations and bubbling phenomena in the riser of three-phase circulation fluidized bed bioreactor with viscous liquid medium were investigated, for the application of this scheme to treat the ammonium component in the wastewater from food processing industries by means of microorganism. The bubble size was measured and dynamic bubbling behaviors in the riser were analyzed by means of the phase space portraits and correlation dimension of the time series of pressure fluctuations.

†To whom correspondence should be addressed.
E-mail: kangyong@cnu.ac.kr

ANALYSIS

1. Phase Space Portraits

The multidimensional phase space portraits can be constructed from the time series of pressure fluctuations by means of the time delay method [22]. That is, the experimentally obtained time-series signal, X(t), is digitized with a time step of Dt; the resultant (m+1) values of the signal, X(i·Δt), are stored for i=0, 1, 2, ..., m. Thus, the vector time series is defined as

$$Z_i(t)=[X(i\cdot\Delta t), X(i\cdot\Delta t+\tau), \cdots, X(i\cdot\Delta t+(p-1)\cdot\tau)],\quad i=0, 1, 2, \cdots, [m-(p-1)\cdot k] \tag{1}$$

where, $\tau=k\cdot\Delta t$, k=1, 2, 3, … and p is the dimension of the vector, Z(t). Therefore, moving along with time t, a series of p-dimensional vectors representing the p-dimensional portrait of the system can be obtained. Occasionally, p is referred to as the embedded phase-space dimension of the reconstructed trajectory of attractor. Actually, if τ=1 and p=3, the state vectors presenting one orbit of attractor are constructed from the experimentally measured time-series signals as $Z_1=[X_1, X_2, X_3]^T$, $Z_2=[X_2, X_3, X_4]^T$, etc. Thus, the number of elements, p, of the state vector is equal to the number of coordinates in the reconstructed state space. In this way a two-dimensional reconstructed attractor of a time series can be obtained.

2. Correlation Dimension

To estimate the correlation dimension of the time series X(t), the trajectories of them reconstructed by resorting to time embedding have been used. From the trajectories of the vector time series the correlation integral (the space correlation function) of the process, C(r), is defined as [23]

$$C(r) = \lim_{m\to\infty}\frac{1}{m^2}[\text{number of pairs (i,j) whose distance } |Z_i(t) - Z_j(t)| < r]. \quad (2)$$

Formally,

$$C(r) = \lim_{m\to\infty}\frac{1}{m^2}\sum_{i=1}^{m}\sum_{j=1}^{m} H[r - |Z_i(t) - Z_j(t)|],\ i\neq j \quad (3)$$

where m is the number of data points, and H is Heavyside function,

$$H[r - |Z_i(t) - Z_j(t)|] = \begin{cases} 1 \text{ if } r > |Z_i(t) - Z_j(t)| \\ 0 \text{ otherwise} \end{cases} \quad (4)$$

The correlation integral, C(r), has been found to be a power function of r for small r's:

$$C(r) = kr^{D_c} \quad (5)$$

The slope of the plot of ln C(r) vs. ln r is an estimate of D_C, which is termed as the correlation dimension, for the given embedded space dimension, p.

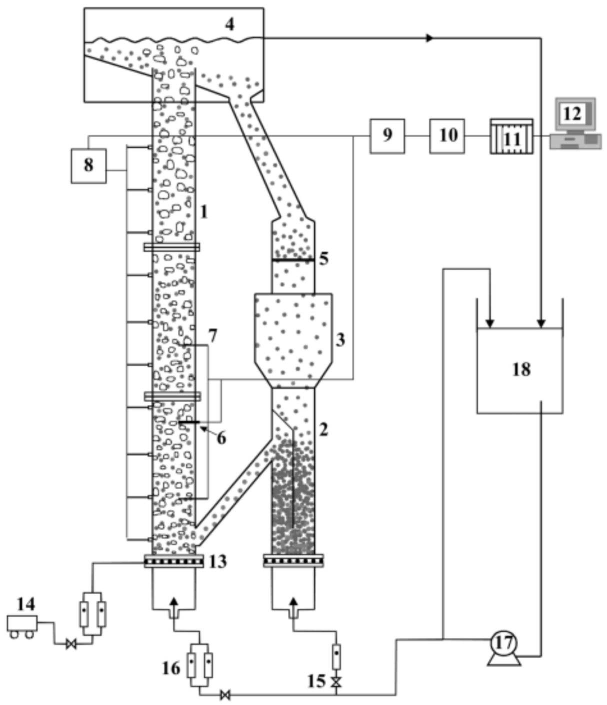

Fig. 1. Experimental apparatus.

1. Riser
2. Down comer
3. Hopper
4. L/S separator
5. Butterfly valve
6. Resistivity probe
7. Pressure transducer
8. Static pressure sensor
9. Amplifier
10. Low-pass filter
11. A/D converter
12. Computer
13. G/L distributor
14. Compressor
15. Control valve
16. Flow meter
17. Pump
18. Liquid reservoir

EXPERIMENTAL

Experiments were carried out in the riser of a three-phase circulation fluidized bed bioreactor which is composed of three main sections, as can be seen in Fig. 1 [15,16]: the riser column, gas-liquid-solid separator and solid recycle device. The diameter and height of the riser was 0.102 m ID and 3.5 m, respectively. A glass bead whose diameter is 1.0 mm (ρ_s=2,500 kg/m^3) was used as a fluidized solid particle, and compressed filtered air was used as a gas phase, respectively. The solid particles were returned to the bottom of the riser through the solid recycle device. The solid circulation rate was 2.0 kg/m^2 sec, which was determined by measuring the amounts of solid piled up above the butterfly valve in the solid recycle device [4,15,16]. The synthesized wastewater, whose compositions are summarized in Table 1, with aqueous solutions of carboxymethylcellulose (CMC), were used as the continuous liquid medium. Recycling activated sludge, which was prepared from a wastewater treatment facility in Wonchun Dong, Daejeon, Korea, was employed as a source of microorganisms. The density and surface tension of the liquid medium were in the range of 1,000-1,003 kg/m^3 and 72.9×10^3-73.6×10^3 N/m, respectively. The characteristics of the pseudoplastic behavior of wastewater were determined by a Brookfield synchrolectric rotational viscometer. In addition, the flow consistency index (K′) and flow behavior index (n) of CMC solution are summarized in Table 2.

The bubble size was measured by means of dual electrical resistivity probe system [4,15,24]. The probe applied by 1.75 V DC detected the difference in conductivity of bubble and liquid. The dual electrical resistivity probe, which was installed at 0.9 m from the inlet of solid recycle device, consisted of two 7 mm diameter stainless steel pipes coated with epoxy resin. The vertical distance between the tips of the probe was 2 mm. The probe was located at the center between the wall and the center of the column. The tips of the probe, which are made of platinum wire, had a diameter of

Table 1. Composition of the concentrated synthetic wastewater

Concentration (g/L)	Component
5.6	Glucose
9.7	$CH_3COONa\cdot 3H_2O$
1.32	KH_2PO_4
0.006	$FeCl_3\cdot 6H_2O$
0.075	$CaCl_2$
2.8	$(NH_4)_2SO_4$
1.0	$MgSO_4\cdot 7H_2O$
0.1098	$MnSO_4\cdot H_2O$
2.1	$NaHCO_3$

Table 2. Liquid physical properties and fluids flow rate range

Solution	ρ_L kg/m^3	K′×10^3 Pa·s^n	n	σ×10^3 N/m	U_G×10^2 m/s	U_L×10^2 m/s
Water	1,000	1.000	1.000	72.9	1.0-7.0	17.0-23.0
CMC(1)	1,001	21.69	0.882	73.2	1.0-7.0	17.0-23.0
CMC(2)	1,002	43.82	0.847	73.3	1.0-7.0	17.0-23.0
CMC(3)	1,003	71.64	0.825	73.6	1.0-7.0	17.0-23.0

0.2 mm. The analog signals obtained from each probe circuit were processed off-line to produce the digital data. The preselected sampling rate at the personal computer with the DT2805 Lab Card was 500 Hz and the total sampling time was 15 s. The bubble size was calculated from the relationship between the reformed and digitized probe signals and the bubble dwell and lag times [11,15]. To avoid noise as well as small disturbances owing to solids, a low-pass filter was used in taking the signals [15,16].

The static and dynamic pressures were measured by means of pressure sensors. A pressure tap for measuring the dynamic pressure fluctuations was mounted flush with the wall of the column in the test section which is located at 1.0 m above the inlet of solid recycle device. To measure the static pressure drop in the reactor, 10 pressure taps were installed at the wall of the column with the intervals of 0.2 m. The pressure sensors were of semiconductor type (Coppel electronics) that have enough fast response time to measure the dynamic pressure fluctuations in the test section. The output voltage from the pressure transducer, which is proportional to the pressure fluctuations or static pressure, was processed by means of a data acquisition system (Data Precision Model, DT3001) and a personal computer. The voltage-time signals, corresponding to the pressure-time signals, were sampled at a rate of 0.005 sec and stored in the data acquisition system. The total acquisition time was 15 sec having 3,000 data points. This combination of sampling rate and time could detect the full spectrum of hydrodynamic signals (200 Hz) in this three-phase circulation flow system [15,16].

RESULTS AND DISCUSSIONS

Typical example of pressure fluctuations in the riser with viscous liquid medium can be seen in Fig. 2. Note that the signals become more irregular and complicated, and the amplitude increases with increasing liquid viscosity. The energy of the periodic behavior in the system can be expressed as the amplitude of pressure fluctuations. Since the density of bubbles is quite different from that of liquid or solid phase, the periodic behavior in the three-phase circulation fluidized-bed reactor can be mainly due to the flow behavior of bubbles. These signals, thus, have been analyzed to examine the bubbling behavior in the riser of the reactor. In Fig. 2, the amplitude of signals tends to increase with increasing viscosity of liquid medium, which implies that the bubble size, D_b, increases with increasing μ_L.

The behavior of pressure fluctuations can be visualized by means of an attractor in the phase space. The phase space portraits of pressure fluctuation signals have been constructed with suitable time lag. The optimum value of time lag has been chosen corresponding to the first minimum in the mutual information function [15,22].

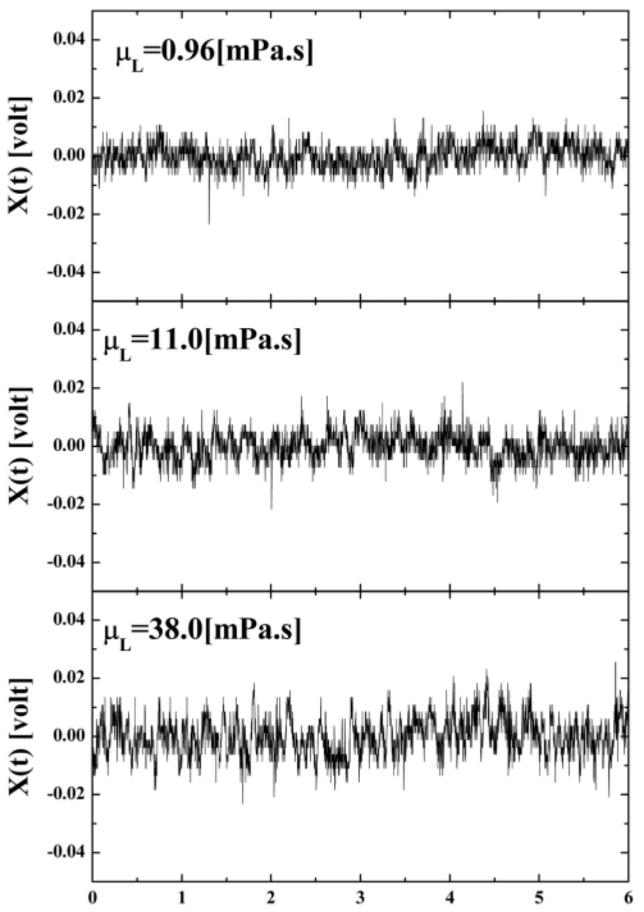

Fig. 2. Typical example of pressure fluctuations in three-phase circulation fluidized bed bioreactors (U_L=0.17 m/s).

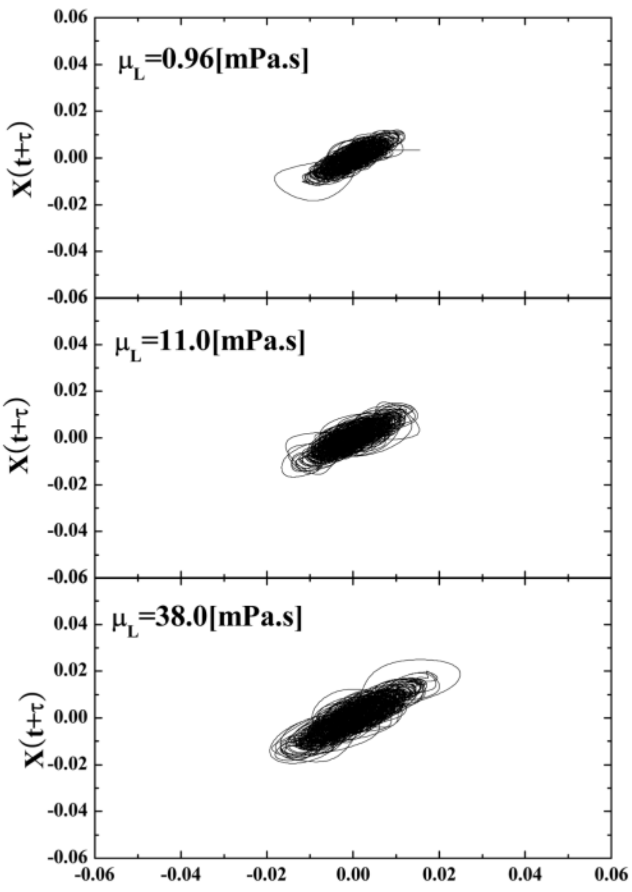

Fig. 3. Phase space portrait of pressure fluctuations in three-phase circulation fluidized bed bioreactors with viscous liquid medium (U_L=0.17 m/s).

Effects of liquid viscosity (μ_L) on the strange attractor of pressure fluctuations can be seen in Fig. 3. The attractor becomes more scattered and complex with increasing μ_L. In comparing the traces of pressure fluctuations with bubble size, it is noted that the scattered traces can be caused by large bubbles, while the small or concentrated traces are smaller bubbles, since the size, location and character of the loops in the trajectories are related directly to the underlying systems with their physical events.

For the quantitative measurement of bubbling behavior in the riser, the correlation dimension of pressure fluctuations has been calculated [23]. The attractor dimension, which can be determined by embedding the trajectories in the phase space, essentially converges with increasing embedding dimension (Fig. 4). From the repeated calculation with different random samples, it has been indicated that the attractor dimension converges when the estimated values are less than 2%. Five or six dimensions of p have been required in the embedding space in order to capture the topological features of the attractor. Effects of liquid viscosity and gas velocity on the correlation dimension of pressure fluctuations can be seen in Fig. 5. In this figure, the D_C value increases with increasing μ_L or U_G, implying that the resultant bubbling behavior becomes more irregular and chaotic with increasing μ_L or U_G in the reactor. This can be mainly due to the variations of bubble size and distribution in the reactor.

The output signals measured by the resistivity probes have been reformed and digitized to produce the digital data from which the bubble size has been calculated [15,16]. The mean value of bubble size has been determined from the logarithmic normal distribution of bubble size, which can be seen in Fig. 6. In this figure, the distribution of bubble size becomes broad and its mean value tends to increase with increasing U_G (Fig. 6A) or μ_L (Fig. 6B). It can be anticipated that the bubble holdup and its frequency increases, which results in the increase of probability of bubble coalescence; thus, the size distribution becomes broad, with increasing U_G. It has been understood that the bubble size becomes increased with increasing μ_L owing to the bubble coalescence in the beds of viscous liquid medium [1,7,8]. The rising behavior of bubbles would be restricted in beds of viscous liquid medium. This can lead to an increase of

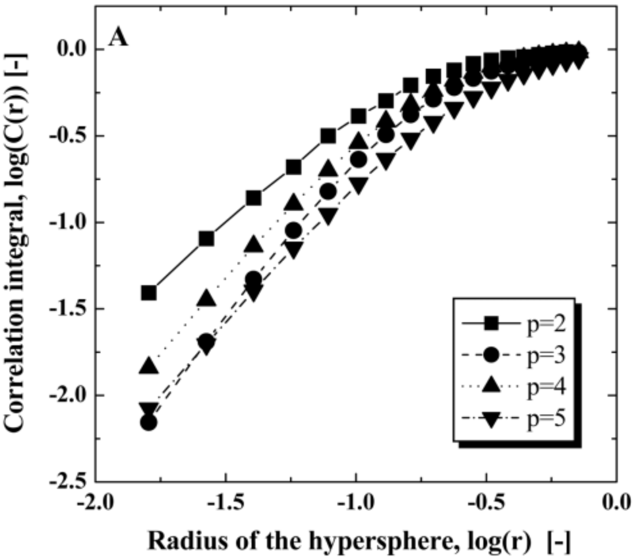

Fig. 4. Typical example of correlation analysis of pressure fluctuations (U_G=0.01 m/s U_L=0.21 m/s μ_L=0.096 mPa·s).

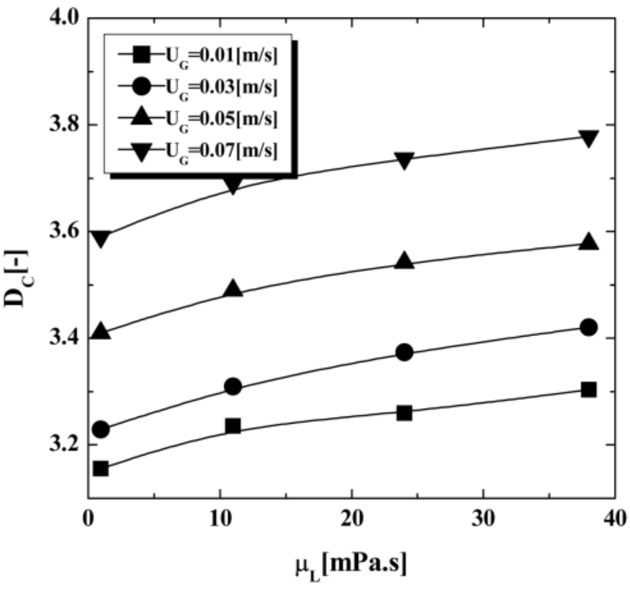

Fig. 5. Effects of μ_L on the correlation dimension of pressure fluctuations in three-phase circulation fluidized bed bioreactors with viscous liquid medium (U_L=0.21 m/s).

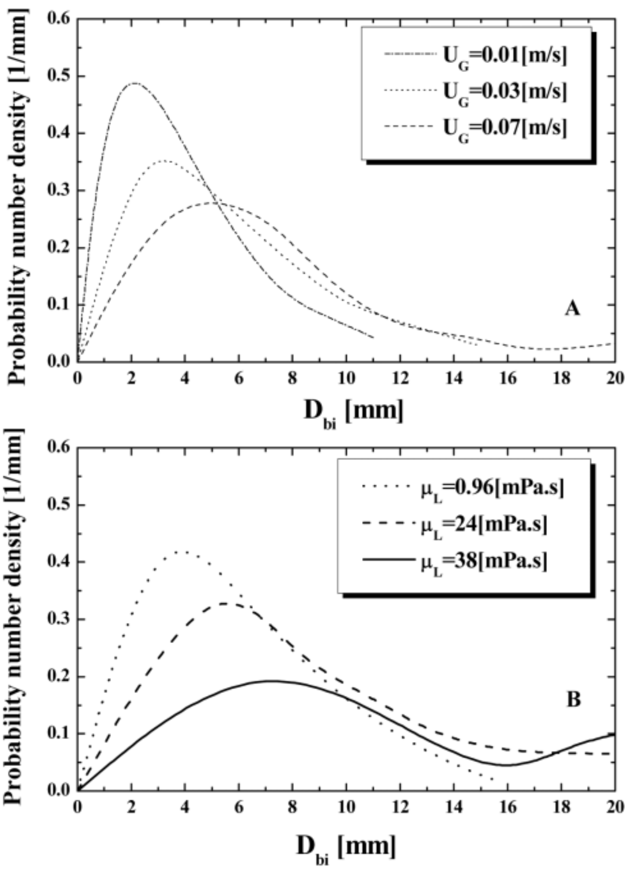

Fig. 6. Probability density of bubble size in three-phase circulation fluidized bed bioreactors with viscous liquid medium (A: U_L=0.23 m/s, μ_L=11 mPa·s, B: U_G=0.01 m/s, U_L=0.19 m/s).

bubble coalescence in a given gas velocity and amount in a reactor.

Effects of U_G on the bubble size can be seen in Fig. 7. In this figure, the bubble size increases with increasing gas velocity. This is due to the increase of gas holdup and frequency with increasing the throughput of gas phase into the riser. It is interesting to note that the bubble size is smaller in the beds with solid circulation than that in the beds of conventional three-phase fluidization [8,15]. This can be attributed to the fact that the turbulence in the bed would increase with increasing liquid velocity, since the U_L value is much higher in the riser of a circulating fluidized bed than that in the conventional three-phase bed. Actually, the bubble size decreases considerably with increasing liquid velocity in the riser with viscous liquid medium, as can be seen in Fig. 8. It has been understood that the bubble flow regime in the beds of 1.0 mm glass beads belongs to the bubble coalescence regime. In other words, the bubble coalescence in the beds is significant owing to the hindrance effects of fluidized particles on the rising bubbles [1,7,8]. But, the increase of U_L results in the increase of rising velocity of bubbles, which leads to a decrease of probability of bubble coalescence in a given amount of bubbles. In addition, the increase of liquid velocity can lead to an increase of turbulence generated in the reactor due to the contacting among gas, liquid and solid phases. Thus, turbulence can act to break down the larger bubbles in the reactor. This consequently results in a decrease of bubble size in the beds.

The bubble size increases gradually with increasing μ_L as can be seen in Fig. 9. It has been known that the increase of μ_L leads to an increase of bubble coalescence [1,8]; thus the bubble size increases with increasing μ_L. However, it can be noted that the increasing trend of D_b with increasing μ_L in the riser of circulation fluidized beds is lower than that in conventional three-phase fluidized beds. This can also be due to the effective turbulence arising from the higher liquid velocity, enough to split the large bubbles in the beds. The bubble size was directly related to the bubbling behavior, which can be represented in terms of pressure fluctuations; thus, it was well correlated with the value of correlation dimension of pressure fluctuations as Eq. (6), with a correlation coefficient of 0.940. In addition, the bubble size was well correlated in terms of dimensionless groups as Eq. (7) based on isotropic turbulence theory, with a correlation coefficient of 0.923.

$$D_b = 0.084 D_C^{2.462} \tag{6}$$

$$\left(\frac{D_b}{d_p}\right) = 36.97\left(\frac{U_G}{U_L + U_G}\right)^{0.249}\left(\frac{\mu_L}{D_V \rho_L}\right)^{0.037} \tag{7}$$

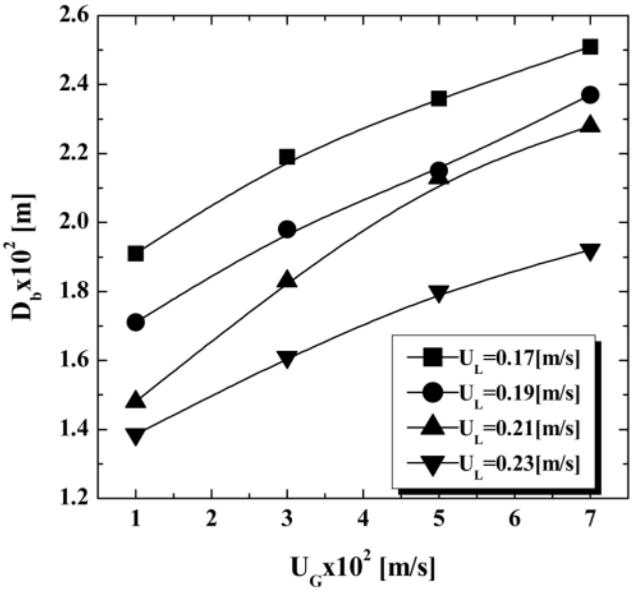

Fig. 7. Effects of U_G on the bubble size in three-phase circulation fluidized bed bioreactors with viscous liquid medium (μ_L= 24 mPa·s).

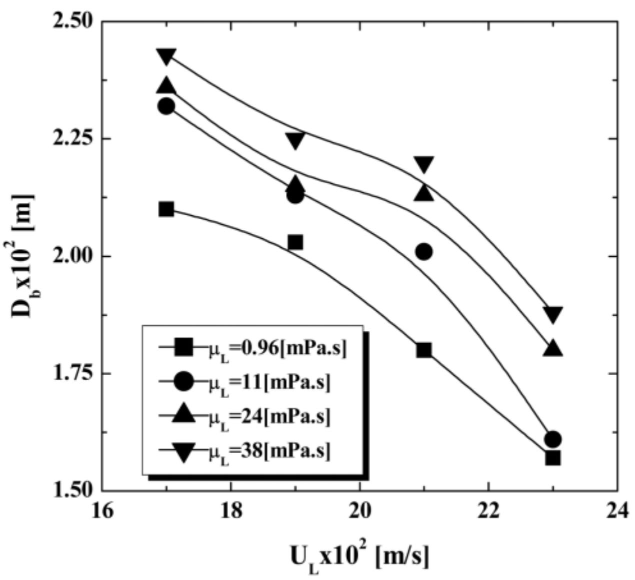

Fig. 8. Effects of U_L on the bubble size in three-phase circulation fluidized bed bioreactors with viscous liquid medium (U_G= 0.05 m/s).

CONCLUSION

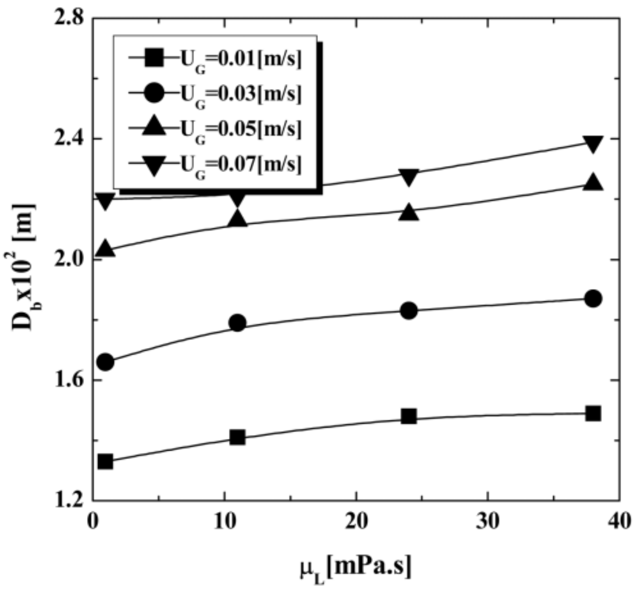

Fig. 9. Effects of μ_L on the bubble size in three-phase circulation fluidized bed bioreactors with viscous liquid medium (U_L= 0.19 m/s).

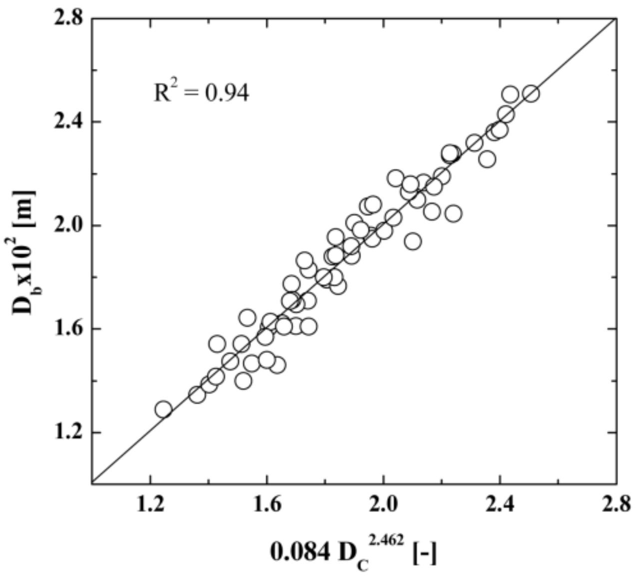

Fig. 10. Relation between the bubble size and the value of correlation dimension of pressure fluctuations.

The bubbling behavior in three-phase circulation fluidized bed bioreactors with viscous liquid medium was successfully interpreted by analyzing the pressure fluctuations and bubble size. The bubble size increased with increasing U_G or μ_L, but decreased with increasing U_L. The uniformity and persistency of bubbling behavior in the riser was related directly to the bubble size; the correlation dimension of pressure fluctuations increased with increasing U_G or μ_L, but decreased with increasing U_L.

The bubble size was well correlated with correlation dimension of pressure fluctuations as well as dimensionless groups as

$$D_b=0.084D_C^{2.462}$$

$$\left(\frac{D_b}{d_p}\right)=36.97\left(\frac{U_G}{U_L+U_G}\right)^{0.249}\left(\frac{\mu_L}{D_V\rho_L}\right)^{0.037}$$

NOMENCLATURE

C(r) : correlation integral
D_C : correlation dimension [-]
D_b : bubble size [mm]
d_p : particle diameter [mm]
D_V : diffusivity [m^2/s]
H : heavyside function
K : constant
K′ : flow consistency index [Pa·s^n]
m : number of data point
n : flow behavior index
p : embedded dimension
r : radius of hypersphere
t : time [s]
U_G : gas velocity [m/s]
U_L : liquid velocity [m/s]
X(t) : time series of pressure fluctuations [V]
Z_i : the vector time series defined as Eq. (1)

Greek Letters

ρ : density [kg/m^3]
ε : holdup [-]
τ : time delay [s]
μ : viscosity [Pa·s]

Subscripts

G : gas phase
L : liquid phase
S : solid phase

REFERENCES

1. L. S. Fan, *Gas-liquid-solid fluidization engineering,* Butterworths: Boston, MA (1989).
2. W. Liang, Q. Wu, Z. Yu, Y. Jin and H. T. Bi, *AIChE J.*, **41**, 267 (1995).
3. W. Liang, Q. Wu, Z. Yu, Y. Jin and Z. Wang, *Can. J. Chem. Eng.*, **73**, 656 (1995).
4. S. H. Kim, Y. J. Cho, P. S. Song, Y. Kang and S. D. Kim, *HWAHAK KONGHAK*, **37**, 961 (1999).
5. J. X. Zhu, Y. Zheng, D. G. Karamanev and A. S. Bassi, *Can. J. Chem. Eng.*, **78**, 82 (2000).
6. S. D. Kim and Y. Kang, *Studies in Surface Science and Catalysis*, **159**, 103 (2006).
7. S. D. Kim and Y. Kang, *Dispersion phase characteristics in three-phase fluidized beds, Mixed flow hydrodynamics*, In N. P. Cheremisinoff Ed., Advances in engineering fluid mechanics series, (pp. 845-869), Houston, Gulf. (1996).
8. S. D. Kim and Y. Kang, *Chem. Eng. Sci.*, **52**, 3639 (1997).
9. C. M. Chen and L. P. Leu, *Chem. Eng. J.*, **81**, 223 (2001).
10. C. M. Chen and L. P. Leu, *Powder Technol.*, **117**, 198 (2001).
11. P. A. Langston, A. S. Burbidge, T. F. Jones and M. J. H. Simmons, *Powder Technol.*, **116**, 33 (2001).
12. T. Wang, J. Wang, W. Yang and Y. Jin, *Powder Technol.*, **137**, 83 (2003)
13. Y. Kang, Y. J. Cho, C. G. Lee, P. S. Song and S. D. Kim, *Can. J. Chem. Eng.*, **81**, 1130 (2003).
14. W. Yang, J. Wang, L. Zhou and Y. Jin, *Chem. Eng. Sci.*, **54**, 5523 (1999).
15. Y. J. Cho, S. H. Nam, S. J. Kim, Y. Kang and S. D. Kim, *Chem. Eng. Sci.*, **56**, 1275 (2001).
16. Y. J. Cho, P. S. Song, S. H. Kim, Y. Kang and S. D. Kim, *J. Chem. Eng. Japan*, **34**, 254 (2001).
17. J. Drahos, F. Bradka and M. Puncochar, *Chem. Eng. Sci.*, **47**, 4069 (1992).
18. K. Kuramoto, A. Tsutsumi and T. Chiba, *Can. J. Chem. Eng.*, **77**, 291 (1999).
19. S. H. Kang, C. G. Lee, P. S. Song, Y. Kang, S. D. Kim and S. J. Kim, *Korean Chem. Eng. Res.*, **42**, 241 (2004).
20. J. S. Kim, S. D. Kim, C. G. Lee, Y. Kang and M. J. Choi, *Korean J. Chem. Eng.*, **21**, 108 (2004).
21. S. M. Son, J. H. Yun, P. S. Song, Y. Kang and S. D. Kim, *Korean Chem. Eng. Res.*, **42**, 235 (2004).
22. A. Fraser and H. L. Swinney, *Physical Review A*, **33**, 1134 (1986).
23. P. Grassberger and I. Procaceia, *Physica D*, **9**, 189 (1983).
24. A. Matsuura and L. S. Fan, *AIChE J.*, **30**, 894 (1984).